Adaptive Sampling of Thermoclines with Autonomous Underwater Vehicles

Nuno A. Cruz and Aníbal C. Matos
INESC Porto and FEUP–DEEC
Rua Dr. Roberto Frias, 4200-465 Porto, Portugal
Email: {nacruz, anibal}@fe.up.pt

***Abstract*— Autonomous Underwater Vehicles (AUVs) are routinely being used to provide the scientific community with detailed ocean data at very reasonable costs. In typical operations, AUVs are programmed to follow pre-defined geo-referenced trajectories, while collecting the relevant information about the underwater environment, with a clear separation between navigation and payload sensors. Under the adaptive sampling paradigm, the AUVs are able to interpret some of the payload data in order to change the sampling pattern and concentrate measurements in the regions of interest. In this paper, we describe an implementation of such paradigm, in which a small sized AUV is able to process CTD data, in real time, and change depth in order to maintain tracking of the thermocline region. We demonstrate the developed algorithms with data from field experiments in a dam reservoir, which show a very good performance, even in very shallow waters with hardly detectable features. The implementation ensures the safety of the AUV, by resuming to standard *yo-yo* patterns if the thermocline is not detected.**

I. Introduction

Autonomous Underwater Vehicles (AUVs) are becoming ordinary tools for ocean sampling, with their mobility and physical autonomy being exploited to achieve wide coverage with minimal setup and operational costs. This yields improvements in efficiency as compared to traditional ocean sampling techniques, particularly when the main objective is to obtain a comprehensive 3-D view of a scalar field. On the contrary, if the objective is to search and map a specific underwater feature, then there is a complex trade-off between the dimension of the search grid, the velocity of the AUV and the total mission duration. This may result in a small percentage of useful data about the specific feature and moderate overall efficiency, which may be further stressed if the feature is dynamic. The concept of *adaptive sampling* has been suggested as a way to address this problem, by processing the environmental data in real time and commanding the AUV to sample the region of interest more densely. Although the concept is very appealing, it was only recently, with the exponential increase in computational power available on-board, associated with more mature software architectures, that there have been a few practical implementations.

One example of the utility of the *adaptive sampling* concept is the characterization of the thermocline – a vertical transition layer on the water column, separating the warm surface layer from the cold deep water bellow it. In a standard approach, the AUV would be programmed to follow a *yo-yo* pattern, resulting in very few data points in the vicinity of the thermocline. Alternatively, the ability to stay within the thermocline region provides more *useful* data, but requires the AUV to process the payload data in real time and adjust the vertical controllers accordingly. In other words, this concept attempts to bridge the gap that usually exists between navigation and payload data. For such an online implementation, it is important to adopt simple models for the feature and to compensate for model inaccuracy by using robust tracking algorithms and overall safety mechanisms.

In a previous work [1], we followed this approach to develop an algorithm for tracking a thermocline, and we have tested it on board the MARES AUV [2], a small sized vehicle developed at the University of Porto, in Portugal (Fig. 1). Using data from a CTD sensor, the AUV was able to detect the thermocline in real time, while moving in a standard *yo-yo* pattern. In this paper, we build on that previous work to increase the tracking performance and the utility of the manoeuver, and we show how our *adaptive sampling* approach can be applied to maintain an AUV in the vicinity of a thermocline, by providing references to the vertical controllers, in real time. We describe the algorithms implemented on board the MARES AUV to guide the vehicle and present quantitative measures of performance that the vehicle computes. Finally, we demonstrate the tracking performance in the field, in a mission where the MARES AUV autonomously adapts the motion pattern to track a thermocline with space and time varying characteristics.

Fig. 1. The MARES AUV with an externally mounted CTD.

II. On-board adaptive sampling

The concept of adaptive sampling in the ocean has emerged with the development of low cost robotic tools with increasing on-line computational power and also with the ability to process large amount of information off-line in a short time. In fact, it is frequent to see *adaptive sampling* identified as the ability to *plan* new missions according to data arriving in real-time from a variety of sources (such as satellite data, CODAR seasondes or meteorological sensors, for example). In [3], for example, both AUVs and research vessels have been programmed to start missions as soon as a given triggering event has occurred. In this work, we consider adaptive sampling as the ability of the vehicle to process payload sensor data in realtime and decide *autonomously* the best trajectory to follow, in order to capture more information about a given oceanographic feature. This concept is sometimes referred to as *real-time adaptive sampling*.

There are many ocean processes that may be efficiently mapped using the adaptive sampling paradigm, particularly if they can be identified by sharp transitions or boundaries. Such efficiency will be accentuated if the processes show high spatial and temporal variations, since the vehicle trajectory can be set to concentrate measurements in the boundary region. Examples of these processes include thermoclines, fronts, eddies, and all sorts of plumes, such as emanating from hydrothermal vents or sewage outfalls.

Even though this is not a new concept, there have been very few practical implementations of real-time adaptive sampling on robotic vehicles. Some successful examples include the use of ROVs to track boundaries on the sea bottom ([4]), and, also, the use of AUVs for searching for the sources of chemical plumes, trying to mimic the real behavior of lobsters or bacterium in odor source localization ([5]–[7]). More recently, there has been some other thermocline tracking experiments, carried out on gliders ([8]) and other AUVs ([9], apart from the authors own implementations ([1]).

One of the main reasons for the shortage of implementations is vehicle safety. In standard AUV operations, the vehicles are programmed to move along geo-referenced trajectories that cover the area of interest. These trajectories are decomposed in sequences of elementary maneuvers, resulting in a *mission plan* to be executed by the on-board software. Although communications perform poorly underwater, there are many solutions for tracking the position of an underwater asset from a remote location and, therefore, it is relatively simple to detect any malfunction just by tracking the position of the AUV during a geo-referenced mission plan. On the contrary, during an adaptive sampling mission, the AUV *decides* the trajectory in real time and the vehicle motion directly depends on mapped features that cannot be easily related with the vehicle dynamics. It is, therefore, difficult to predict the vehicle motion and also to devise simple mechanisms to detect malfunctions and ensure the safe operation of the AUV.

In our case, we have followed a conservative approach to adapt the onboard software architecture of the MARES AUV

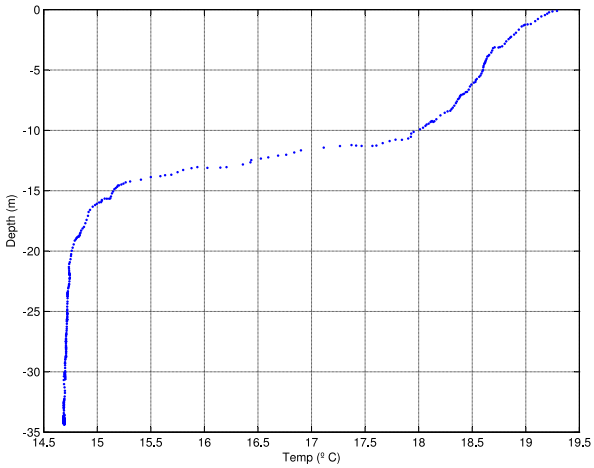

Fig. 2. Temperature profile measured 2 km off the Portuguese coast, June 2009. The thermocline can be easily identified at about 11-14 meters of depth.

[2] to include the capability of real time adaptive sampling. The adaptive sampling maneuvers simply define reference inputs for the already existing real time controllers. This way, when an adaptive sampling maneuver is activated, the reference inputs for the control system are computed in real time by dedicated modules of software (that implement the adaptive sampling behaviors) and are fed to the controllers. In the particular case of thermocline tracking, the algorithm provides in real time the depth reference for the vertical controller, based on the acquired CTD data, as explained later. In any case, a protection layer of the control system sets limits for the reference values provided by the external modules, preventing the vehicle to enter unwanted regions and ensuring safety of operation.

III. Application scenario – The thermocline

In this work, we consider the scenario of detection and characterization of a thermocline in a given region. The thermocline is the transition layer in the water column that separates the warmer surface water from the cold deep water. The so-called *mixed layer*, closer to the surface, is the most easily influenced by atmospheric conditions (wind, rain and solar heat), resulting in a wide range of values throughout the year, while the deep-water layer is the less dynamic zone, with a slow variation with depth. In the thermocline, the water temperature drops as the depth increases, with a significant gradient as compared to the rest of the profile. Figure 2 shows an example of a temperature profile measured 2km off the Portuguese coast, in about 40m of water.

The thermocline can be permanent or seasonal and may develop both at sea [10] or in inner waters such as lakes and dam reservoirs [11]. The characterization of the thermocline is particularly relevant to marine biology, since the location and variability of the characteristics can provide valuable information about phytoplankton concentration and primary production [12]. The thermocline is also associated to water stratification, with strong impact on underwater acoustics and,

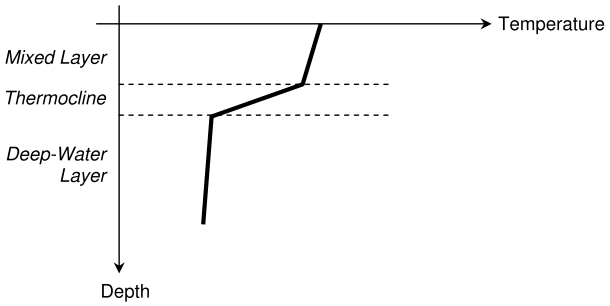

Fig. 3. Simplified temperature profile.

therefore, its characterization can play an important role in underwater communications and military strategic planning. By *characterization*, we mean to gather enough data to provide a quasi-synoptic 4-D view of the thermocline.

Temperature is probably the most measured parameter in all water masses and given the huge amount of data that exists about the world oceans, there have been several attempts to represent these temperature profiles by simple sets of coefficients, in order to reduce the data warehousing requirements. This effort has been helped by the relatively regular *shape* of the profiles, that suggests a parametric representation. In any case, the proposed parametric models (for example [13]–[16]) require the availability of the full temperature profile to extract the parameters. Note that our idea is not to provide a very accurate model that approximates the true vertical profiles, minimizing some optimization criteria, but, instead, our main concern is that the model is simple enough to be iteratively estimated in real time. Even with only a partial vertical profile, the AUV has to be able to determine its main characteristics and maintain a trajectory in the vicinity of the thermocline. In order to achieve this, we assume a 3-layer piecewise linear model, similar to the one proposed by Haeger [13], with a high gradient at the thermocline, and low gradients both above and below. Figure 3 shows such a representation, where the three vertical zones can be easily identified.

IV. The Thermocline Tracking Maneuver

Overview

The current implementation of the thermocline tracking maneuver is the evolution of the first implementation, described in [1]. In this paper, we will only focus on the main characteristics of the maneuver and the new features, which can be summarized as:

- all parameters are computed on line, requiring no *a-priori* estimation of the thermocline;
- the thermocline tracking manoeuver has been extended to include additional parameters adjusted to the objectives for the mission (for example, extend the vertical span downwards to map possible chlorophyll or phytoplankton patches below the thermocline);
- An auto-diagnosis performance index is computed in real time and transmitted to a mission supervisor.

The thermocline tracking maneuver acts directly on the vertical controllers of the AUV, requiring a set of values for depth limits, which can be defined with respect to the surface or the bottom. In case the thermocline is not detected, the vertical motion of the AUV reverts to a standard *yo-yo* between those values. A specific process runs in the onboard computer, identifying the thermocline, filtering temperature data and fitting a gradient search algorithm implemented in real time. The thermocline is detected when the vertical temperature gradient exceeds a given threshold. The vehicle will proceed the vertical motion until the algorithm detects a *significant decrease* in the gradient, as compared to the current *maximum*. At this position, the vertical profile is reversed and the algorithm restarts on the other direction. In the absence of a positive identification of the thermocline in either direction, then the vehicle will continue the vertical motion until the prespecified limit is reached (either the surface or the maximum depth), as in a standard *yo-yo* motion. All thresholds are dynamic and depend on the gradient information acquired on previous profiles, so that the AUV can be used to track a time- or space-varying thermocline while moving along a predefined *lat-lon* trajectory.

During the thermocline tracking maneuver, the model parameters can be passed on to other AUV processes, if necessary, in the same way as the references are passed on to the controllers. This allows, for example, the AUV to switch on any special sensor or to trigger an underwater sampler at the right instant, in order to capture a relevant sample of water for laboratory analysis, such as suggested in [17].

Tracking the thermocline

The algorithm developed for thermocline tracking can be described by the state machine represented in fig. 4, where the dark arrows represent the transitions that are expected during a successful tracking. These transitions will cycle the state machine through the most relevant states:

- TOP - The vehicle is located above the thermocline.
- TC2BOT - The AUV is within the region of the thermocline, on a downward vertical motion.
- BOTTOM - The vehicle is located below the thermocline.
- TC2TOP - The AUV is within the region of the thermocline, on an upward vertical motion.

Note from the state machine that there are only 2 possibilities for the depth reference (Z_{ref} is either Z_{min} or Z_{max}) and it only changes whenever the TOP or BOTTOM states are reached. During a dive, the AUV will evaluate the vertical temperature gradient and compare it with a given threshold, Thr_tc. When this threshold is exceeded, the vehicle will assume the thermocline has been detected on the downward motion, entering the TC2BOT state. This can be seen as the *upper limit* of the thermocline region and then the vehicle will try to detect the *lower limit* of this region, by diving deeper. Therefore, the vertical direction will remain the same as before and the gradient search algorithm will try to find if the level decreases below another threshold, Thr_bot. In order to confirm the *lower limit* of the thermocline and avoid (early)

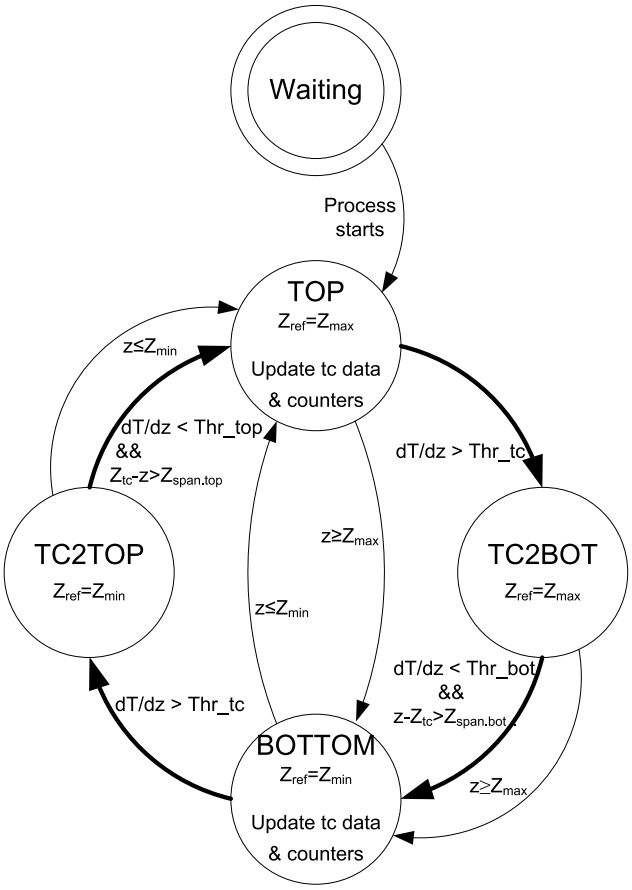

Fig. 4. State machine and transitions representing the thermocline tracking maneuver. The bold arrows represent the expected cyclic transitions during normal tracking.

false detections, an additional test is performed, verifying that the vertical span is large enough, *i.e.* if $z - Z_{tc} > Z_{span.bot}$, where z is the current depth, Z_{tc} is the depth of the maximum gradient and $Z_{span.bot}$ is an optional parameter set by the user to extend the vertical range downwards and allow for data collection below the thermocline. When both these conditions are met, the vehicle enters the BOTTOM state.

Note from the state machine of fig. 4 that the BOTTOM state is also reached if $z \geq Z_{max}$, which is a safety mechanism to ensure that the maximum depth the AUV will be limited to Z_{max}, even if the algorithm is not able to positively *find* the *upper limit* or the *lower limit* of the thermocline. When the vehicle enters the BOTTOM state, the thermocline characteristics are extracted from the previous vertical profile (in particular, the maximum gradient and the thermocline limits) and this information is used to adapt the thresholds for the thermocline detection during the next vertical profile. The depth reference changes to Z_{min}, which means the AUV will now move towards the surface, and the algorithm will proceed in much the same way as in the downward motion.

As long as this process is active, the above cycle will be maintained, resulting in a *yo-yo* pattern around the thermocline. It should be noted than on the very first time the algorithm runs (usually during the first descend), it is possible either to use *a priori* data to define the initial detection thresholds, or to use no information at all and let the AUV acquire a full vertical profile to determine those values.

Performance index

In order to evaluate the performance of the algorithm, a simple mechanism is to maintain 3 different counters that are increased depending on the state transitions that lead to the reversal of the profiles (TOP and BOTTOM states). The first counter, **full_track**, is increased when the vehicle detects both the beginning and the end of the thermocline, *i.e.* reaches the TOP or BOTTOM states through a dark arrow; the second, **begin_only**, is increased when the vehicle enters a transition state (TC2TOP or TC2BOT) but does not detect the end of the thermocline. Finally, a third counter, **fail**, is increased if there is a direct transition from the TOP to the BOTTOM, or vice-versa.

Practical implementation issues

In order to estimate the temperature gradients, we cluster data points into bins and take the differences of the averaged values. The size of the bins is adjusted dynamically according to the thickness of the thermocline, the vertical velocity of the AUV and the sampling rate of the CTD. The size of the depth bins acts as a low pass filter which may affect the ability to detect gradients. Smaller bins result in large errors in gradient estimation, while larger bins smooth the temperature variations and hinder the separation of gradients. After testing with both real and simulated vertical temperature profiles, we've had good results with at least 5 to 8 bins spanning the depths of the thermocline. As a rule of thumb, we usually set this value so that the first estimated thermocline spans about 10 bins.

Even with the clustering of data into bins, there may exist some false detections of gradients if we only consider a single bin at a time. In order to avoid these false detections, we've considered a minimum number of 3 consecutive detections to confirm the gradient thresholds. We've also implemented a mechanism of validating a bin, depending on the quantity of data points used. For our experiments, we've considered a minimum number of 5 data points in a bin for its data to be used for gradient detection.

During normal tracking, the transitions between states are triggered by the detection of temperature gradients above or below specific thresholds. These thresholds are updated for each new profile, to allow for temporal and spatial variations of the thermocline parameters, but this choice may have a strong impact on the algorithm performance. In our case, we define the threshold for the thermocline of a new profile (Thr_tc) to be 50% of the maximum gradient found in the previous profile. Typical temperature profiles exhibit more variation towards the surface than towards the bottom and therefore we set Thr_top= $1/2\times$Thr_tc and Thr_bot= $1/4\times$Thr_tc.

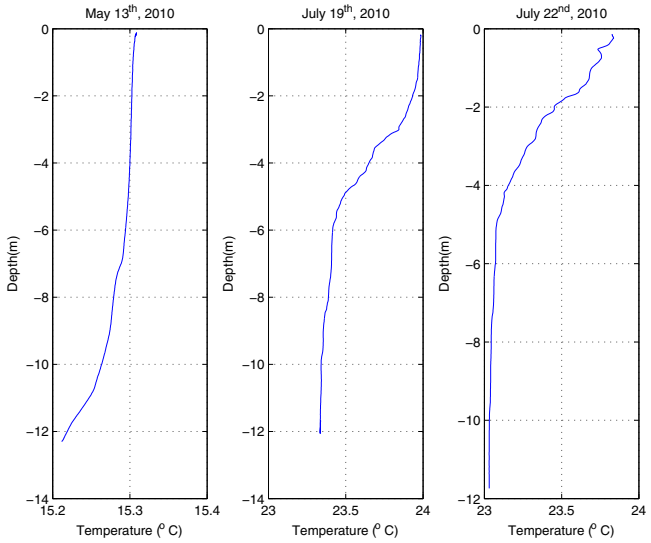

Fig. 5. Temperature profiles measured by the MARES AUV at approximately the same location of the Crestuma reservoir. The thermocline is visible in the summer profiles, reaching the surface in the last plot.

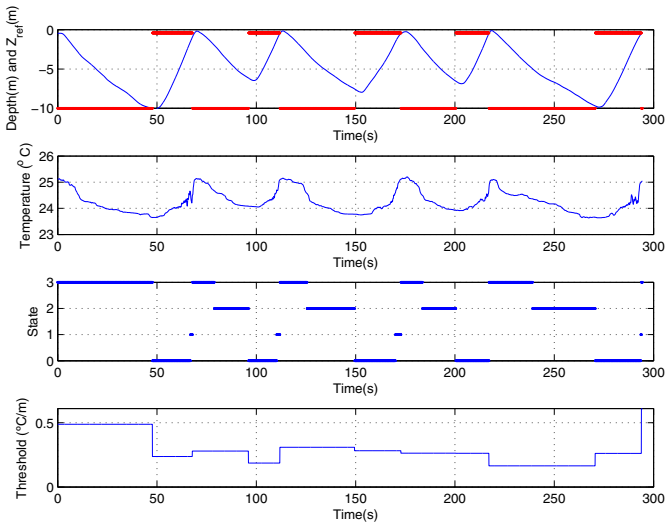

Fig. 6. MARES AUV tracking a thermocline in the Crestuma reservoir, August 2010. The first plot shows the depth of the vehicle in blue and the depth reference in bold-red. The states of the third plot correspond to: TOP (3), TC2BOT (2), BOTTOM (0), and TC2TOP (1).

V. Field tests and results

After demonstrating the capability of tracking the thermocline by simulation, using data from previous AUV profiles, we moved on to the validation in the field, using the thermocline tracking maneuver in a set of field trials carried out with the MARES AUV in a dam reservoir in the Douro river, close to Porto, in the north of Portugal, during the summer of 2010. This site is an appropriate location to demonstrate the maneuver, since it is known to develop seasonal thermoclines from late spring to early autumn, with significant spatial and temporal variations. From the examples in fig. 5 it is clear that the thermocline is much less pronounced that the thermoclines typically found in the ocean, even in costal waters (for example, in fig. 2). It is also clear that the reservoir thermocline has much more small-scale variations, particularly in the mixed layer, above the thermocline. For the thermocline tracking algorithm, this provides a much harder scenario than a smooth variation and, therefore, it is a good way of demonstrating its effectiveness.

As far as logistics are concerned, the site is very close to our lab (just a 30-minute drive) and we have access to a small motor-boat to support operations. We used this boat to deploy 2 buoys with acoustic beacons, located 350m apart, which provided a baseline for acoustic navigation of the AUV and tracked the vehicle position in real time. The MARES AUV has 4 independent controllers for 4 degrees of freedom, and the vehicle is able to control the vertical velocity, from zero (*i.e. hovering*) to a maximum value around 40cm/s. This means that the vehicle can implement this algorithm to track the vertical thermocline at a single *lat-lon* location, or while following a completely independent *horizontal* trajectory. During the first trials we tried the thermocline tracking maneuver without any horizontal motion, but the performance was very dependent on the location of the AUV, since in some regions of the dam there was an almost linear variation of temperature from the surface to the bottom. We then changed the mission plan, so that the AUV was programmed to follow a *lat-lon* trajectory, diagonally in the river, trying to capture the thermocline. Given the shallowness of the river (10–15 meters), we've set the upper and lower limits to 0.5 and 10 meters, respectively. Note that at this time we did not have any altimeter on board, otherwise we could have set the lower limit to be an offset above the bottom.

Fig. 6 shows the details of one of the missions, with a total of 10 profiles in about 300 seconds (and roughly 300 meters of horizontal range). Note in the first plot the depth reading during the *yo-yo* motion and the solid red line indicating the depth reference provided by the thermocline tracking algorithm. The states of the algorithm state machine correspond to the earlier description: TOP (3), TC2BOT (2), BOTTOM (0), and TC2TOP (1). The last plot shows the evolution of the thermocline threshold as the new profiles are completed.

In terms of practical results, the performance counters ended up this trajectory with: **full_track**=5, **beg_only**=3, and **fail**=2. If we take out the first dive (used to provide the algorithm with initial data), this means that in 8 out of the other 9 profiles, the vehicle was able to detect the thermocline. This corresponding to the *yo-yo* pattern seen in fig. 6, during the interval between 50 and 275 seconds, even though in 2 of these profiles, the vehicle almost reached the limits (at approximately 70 and 275 seconds). The plots of figure 7 show some of the T-D profiles that were tracked during this period and they stress the difficulty in tracking, since the thermoclines extend almost to the surface and show very low gradients.

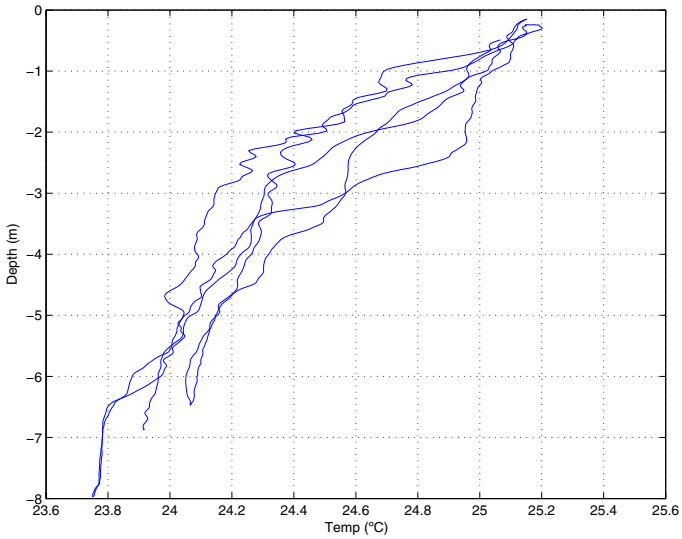

Fig. 7. Some of the T-D profiles tracked during the demonstration mission, taken during to the interval 50–275 s.

VI. Conclusions and Future Work

The MARES onboard software architecture was adapted to incorporate the capability of real time adaptive sampling, providing a framework to implement innovative guidance algorithms that infer some characteristics of the oceanographic environment and react to this environment by making decisions about the best sampling strategy to use. We envisage that such framework may be usefull not only to track a space- and time-varying thermocline, as demonstrated in this papers, but also to efficiently characterize other ocean processes under the same paradigm.

The thermocline tracking maneuver has been employed on board the MARES AUV in a very difficult scenario, with significant small-scale variations, very low separation between surface and bottom temperatures (about 1^oC) and maximum gradients in the range 0.2–0.3^oC/m. The results demonstrated an excellent tracking performance and also showed that the algorithm was implemented in such a way as to ensure safety of operation – in the cases the algorithm was not able to positively detect the thermocline, then the AUV reverted to a standard *yo-yo* pattern.

As far as the thermocline tracking is concerned, we plan to improve the real time filtering of the parameters of the algorithm, so that the tracking mechanism may benefit more from the results of previous profiles, such as thermocline depth limits, detection thresholds, and temperature levels both above and below the thermocline. We also plan to evaluate the correlation between the thermocline characteristics and other ocean data, such as chlorophyll concentration, for example, in order to improve the tracking mechanism by incorporating more information.

References

[1] N. Cruz and A. Matos, "Reactive AUV motion for thermocline tracking," in *Proc. IEEE Int. Conf. Oceans'10*, Sydney, Australia, May 2010.

[2] ——, "The MARES AUV, a modular autonomous robot for environment sampling," in *Proc. MTS/IEEE Int. Conf. Oceans'08*, Quebec, Canada, Sept. 2008.

[3] O. Schofield, T. Bergman, P. Bisset, J. F. Grassle, D. B. Haidvogel, J. Kohut, M. Molin, and S. M. Glenn, "The long-term ecosystem observatory: An integrated coastal observatory," *IEEE J. Oceanic. Eng.*, vol. 27, no. 2, pp. 146–154, Apr. 2002.

[4] C. Barat and M. J. Rendas, "Benthic boundary tracking using a profiler sonar: A mixture model approach," in *Proc. MTS/IEEE Int. Conf. Oceans'03*, San Diego, CA, USA, Sep. 2003, pp. 1409–1416.

[5] J. A. Farrell, W. Li, S. Pang, and R. Arrieta, "Chemical plume tracing experimental results with a REMUS AUV," in *Proc. MTS/IEEE Int. Conf. Oceans'03*, San Diego, CA, USA, Sep. 2003, pp. 962–968.

[6] S. Pang and J. A. Farrell, "Chemical plume source localization," *IEEE Trans. Syst., Man, Cybern. B*, vol. 36, no. 5, pp. 1068–1080, Oct. 2006.

[7] W. Naeem, R. Sutton, and J. Chudley, "Chemical plume tracing and odour source localization by autonomous vehicles," *The Journal of Navigation*, vol. 60, no. 2, pp. 173–190, May 2007.

[8] H. C. Woithe and U. Kremer, "A programming architecture for smart autonomous underwater vehicles," in *Proc. IEEE/RSJ Int. Conf. Intelligent Robots and Systems IROS'09*, St. Louis, MO, USA, Oct. 2009.

[9] S. Petillo, A. Balasuriya, and H. Schmidt, "Autonomous adaptive environmental assessment and feature tracking via autonomous underwater vehicles," in *Proc. IEEE Int. Conf. Oceans'10*, Sydney, Australia, May 2010.

[10] G. L. Pickard and W. J. Emery, *Descriptive Physical Oceanography – An Introduction*, 5th ed. Pergamon Press, 1990.

[11] B. M. Johnson, L. Saito, M. A. Anderson, P. Weiss, M. Andre, and D. G. Fontane, "Effects of climate and dam operations on reservoir thermal structure," *J. Water Resour. Plann. Manage.*, vol. 130, no. 2, pp. 112–122, Mar./Apr. 2004.

[12] J. Sharples, "Investigating the seasonal vertical structure of phytoplankton in shelf seas," *Mar. Model.*, vol. 1, no. 1–4, pp. 3–38, 1999.

[13] S. D. Haeger, "Vertical representation of ocean temperature profiles with a gradient feature model," in *Proc. MTS/IEEE Int. Conf. Oceans'95*, San Diego, CA, USA, Oct. 1995, pp. 579–585.

[14] P. C. Chu, Q. Wang, and R. H. Bourke, "A geometric model for the Beaufort/Chukchi Sea thermohaline structure," *J. Atmos. Oceanic Technol.*, vol. 16, no. 6, pp. 613–632, Jun. 1999.

[15] P. C. Chu, C. Fan, and W. T. Liu, "Determination of vertical thermal structure from sea surface temperature," *J. Atmos. Oceanic Technol.*, vol. 17, no. 7, pp. 971–979, Jul. 2000.

[16] V. Babovic and H. Zhang, "Modeling of vertical thermal structure using genetic programming," in *Proc. 7th OMISAR Workshop on Ocean Models*, Singapore, Sep. 2002. [Online]. Available: http://sol.oc.ntu.edu.tw/OMISAR/wksp.mtg/WOM7/1.pdf

[17] Y. Zhang, R. S. McEwen, J. P. Ryan, and J. G. Bellingham, "An adaptive triggering method for capturing peak samples in a thin phytoplankton layer by an autonomous underwater vehicle," in *Proc. MTS/IEEE Int. Conf. Oceans'09*, Biloxi, MI, USA, Oct. 2009.